Template for Preparation of Manuscripts for *Nano Research*

This template is to be used for preparing manuscripts for submission to *Nano Research*. Use of this template will save time in the review and production processes and will expedite publication. However, use of the template is not a requirement of submission. Do not modify the template in any way (delete spaces, modify font size/line height, etc.). If you need more detailed information about the preparation and submission of a manuscript to Nano Research, please see the latest version of the Instructions for Authors at http://www.thenanoresearch.com/.
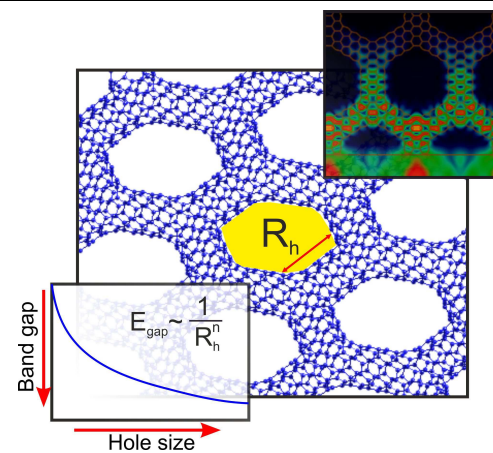
TABLE OF CONTENTS (TOC)

Authors are required to submit a graphic entry for the Table of Contents (TOC) in conjunction with the manuscript title. This graphic should capture the readers' attention and give readers a visual impression of the essence of the paper. Labels, formulae, or numbers within the graphic must be legible at publication size. Tables or spectra are not acceptable. Color graphics are highly encouraged. The resolution of the figure should be at least 600 dpi. The size should be at least 50 mm × 80 mm with a rectangular shape (ideally, the ratio of height to width should be less than 1 and larger than 5/8). One to two sentences should be written below the figure to summarize the paper. To create the TOC, please insert your image in the template box below. Fonts, size, and spaces should not be changed.

Bilayered semiconductor graphene nanostructures with periodically arranged hexagonal holes

Dmitry G. Kvashnin*, Péter Vancsó, Liubov Yu. Antipina, Géza I. Márk, László P. Biró, Pavel B. Sorokin, Leonid A. Chernozatonskii*

Emanuel Institute of Biochemical Physics, Moscow, Russia
Institute of Technical Physics and Materials Science, Research Centre for Natural Sciences, Budapest, Hungary
Technological Institute of Superhard and Novel Carbon Materials, Troitsk, Moscow, Russia

In this work the novel hexagonal nanomeshes based on bilayered graphene were studied. Electronic and transport properties and the dependences of the band gap on two main parameters characterizing the geometry were studied in detail.

Provide the authors' webside if possible.
Author 1, webside 1
Author 2, webside 2

TSINGHUA UNIVERSITY PRESS Springer

Bilayered semiconductor graphene nanostructures with periodically arranged hexagonal holes

Dmitry G. Kvashnin[1]($\boxtimes$),Péter Vancsó[2], Liubov Yu. Antipina[3], Géza I. Márk[2], László P. Biró[2], Pavel B. Sorokin[1,3] and Leonid A. Chernozatonskii[1]($\boxtimes$)

[1] Emanuel Institute of Biochemical Physics, 4 Kosigina Street, Moscow, 119334, Russia

[2] Institute of Technical Physics and Materials Science, Research Centre for Natural Sciences, H-1525 Budapest, P.O., Hungary

3 Technological Institute of Superhard and Novel Carbon Materials, 7a Centralnaya Street, Troitsk, Moscow, 142190, Russia

ABSTRACT

We present a theoretical study of new nanostructures based on the bilayered graphene with periodically arranged hexagonal holes (bilayered graphene antidots). Our *ab initio* calculations show that fabrication of hexagonal holes in bigraphene leads to connection of the neighboring edges of the two graphene layers with formation of a hollow carbon nanostructure sheet which displays wide range of electronic properties (from semiconductor to metallic), depending on the size of the holes and the distance between them. The results were additionally supported by wave packet dynamical transport calculations based on the numerical solution of the time-dependent Schrödinger equation.

INTRODUCTION. Graphene, a two-dimensional (2D) carbon crystal with honeycomb structure was first isolated by the micromechanical cleavage of graphite in 2004. [1,2] Beside the monolayer film, bilayered graphene attracts a specific attention due to its particular electronic properties. [3] Like in the case of monolayer, the bilayered graphene is semimetal, but its conduction and valence bands touch with quadratic dispersion, opposite to the linear dispersion relation seen in one layer graphene. [4] Therefore, the problem of the lack of a semiconductor band gap remains in bilayered graphene. The fabrication of bilayered graphene ribbons or adsorption of adatoms to bilayered

graphene structure, like in the case of single layer graphene, [5-7]can open a band gap, but also create scattering regions whereas it is highly desirable to avoid the depression of mobility of the π-electrons. It is possible to open a gap using electric field effect, [8] but its size is tiny, and cannot be used in semiconductor devices.

A promising way to open a band gap in graphene is the making of periodical nanopores in the structure. It was predicted that such periodic arrays of holes in graphene lattice transform graphene from semimetal to semiconductor with a tunable band gap by means of the changing of the period and the size of the holes. [9-11] Periodical nanopores were experimentally realized by different methods, [12-16] with general confirmation of theoretical predictions. [9,10,17-20] The transport measurements show that such materials display an effective energy gap (~100 meV) and an ON-OFF ratio up to 10, which is a promising feature of the graphene antidot scheme. [21,22] It can be speculated that while in the case of a graphene monolayer such holes act as scattering edges, in the case of a bilayered structure the neighboring graphene edges can connect with each other (as was shown in several experimental papers on formation of a closed-edge structure [23-26] after an e-beam irradiation of the bilayered graphene). This would create a bilayer hollow graphene material without edges, i.e. without any interruption of the sp^2 carbon lattice. Such kind of structures with closed-edges can be described as a complex structure that combines the flat geometry of graphene with the curvature of small diameter nanotubes. Curvature effects induce local hybridization, which can bring new physics, which is able to give a new opportunity to apply bigraphene-based nanostructures in nanoelectronic devices. A further advantage may be that while the building of a regular carbon nanotube lattice from individual CNTs seems presently less feasible, a regular structure resembling such lattice may be produced by the coupling of the atomic bonds at the edges of bilayered graphene antidote lattice.

Here we will show that creating of holes in bilayered graphene leads to the formation of a family of novel closed-edge hollow nanostructures with special electronic properties. We found that the highly strained edges of the bilayered graphene holes tend to compensate dangling bonds by the stitching of the edges of the two layers. We investigated the electronic properties of these superlattices with hexagonal unit cell and obtained that depending upon the atomic geometry (the size of the holes and the distance between them) both semiconducting (with band gap ~1 eV) and metallic behavior can occur. The propagation of the electrons was also studied using a wave packet dynamical (WPD) transport approach.

The organization of the paper is a follows. In Sec. 2 the calculation methods are presented. Section 3 consists of three parts. The first part gives the results of the investigation of the stability and formation of bilayered graphene superlattices (BGS) with connected layers and hexagonal holes. In the second part of Sec. 3 the investigation of the electronic properties depending on the geometric parameters was performed and the origin of the specific electronic properties was discussed. The third part is devoted to the calculation of the transport properties. Sec. 4 contains the discussion of the results.

CALCULATION METHODS. The investigation of the geometry and stability of the BGS were made from an energetic point of view using the density functional theory with local density approximation (DFT-LDA) implemented in SIESTA package with periodic boundary conditions. [27] To calculate equilibrium atomic structures, the Brillouin zone was sampled according to the Monkhorst-Pack [28] scheme with a k-point density of 0.08 Å^{-1}. In the course of the atomic structure minimization, structural relaxation was carried out until the change in the total energy was less than 10^{-4} eV, or forces acting on each atom were less than 10^{-3} eV/Å. The number of atoms in hexagonal unit cell was 150 to 1000, depending on structural parameters.

The electronic properties were calculated using the DFTB approach, [29] with a second-order expansion of the Kohn-Sham total energy in density functional theory with respect to charge density fluctuations implemented in DFTB+ software package. This method can provide the qualitative data about the changes of the value of the band gap. This method is well-established to describe the complex properties of materials. [29] The band structures were constructed with set of k-points from 20 to 5 depending on the size of unit cell in each of the

high-symmetry directions.

We performed transport calculations of the modelled BGS by using wave-packet dynamics (WPD), [30] which is able to handle systems containing a large number of C atoms compared to the *ab-initio* calculations. Further advantage of the WPD method is that it makes it possible to identify the scattering sites responsible [31] to the characteristic features in transport functions.

In our geometry, the wave packet (WP) is injected from a metallic electrode to the semi-infinite structure modeling a transport measurement setup. The metallic electrode is approximated by a jellium potential with Fermi energy $E_f = 5$ eV and work function $W = 4.81$ eV. For the considered BGS, we used a local one-electron pseudopotential [32] matching the band structure of graphite and graphene sheet. This parameterized potential

$$V(\vec{r}) = \sum_{j=1}^{N} \sum_{i=1}^{a} A_i e^{a_i |\vec{r}-\vec{r}_j|}$$, where $\vec{r}_j$ denote the

atomic positions and N is the number of the atoms, has also been successfully applied for carbon nanotubes [33] and graphene grain boundaries. [34] The incoming wave packet from the electrode was launched with $E_k = E_F = 5\,eV$ kinetic energy and had a spatial width of $\Delta y = 0.37\,nm$, $\Delta x = \Delta z = \infty$. The time development of the wave packets were calculated using a modified version of our computer code developed for solving the time-dependent Schrödinger equation for carbon nanotubes and graphene. [35,36]

RESULTS AND DISCUSSION. Here we considered BGS in which the hexagonal holes have zigzag edges. Such type of edges was chosen based on experimental data [13,37] where holes with dominantly zigzag edges was obtained after the graphene etching. Moreover, according to theoretical predictions armchair edges of bilayered graphene cannot form a closed structure due to geometrical incompatibility. [26] Due to the high in-plane elastic constant and small bending modulus graphene tends to minimize edge energy by out-plane bending (if it can). This effect is responsible for the bending of narrow graphene nanoribbons with bare edges. [23,38] Whereas in the case of a graphene monolayer the edges display dominantly an in-plane reconstruction, the presence of highly strained edges

of the neighboring layers in BGS leads to the bending and connection of the two edges to compensate dangling bonds (the same behavior was observed in bigraphene edges, see Refs [24-26]). Therefore, the creation of the periodically arranged holes in bigraphene should lead to fabrication of hollow carbon structures with closed edges, as illustrated in *Figure 1* a-b. We found that such a process runs without any activation barrier (*Figure 1* c) for any of the structures considered in this work, and therefore we can expect that during an experiment such a structure will be formed spontaneously.
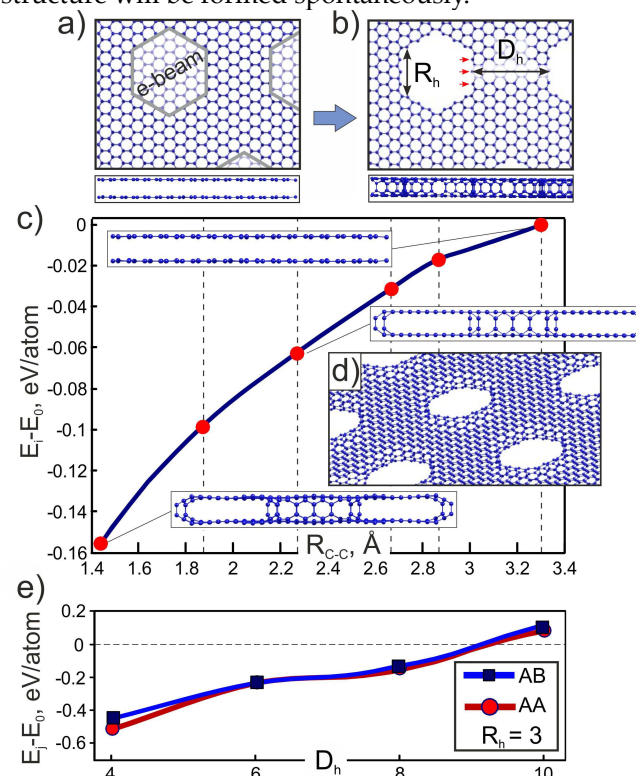

Figure 1 The proposed scheme of fabrication. (a) Top and side view of the pristine structure of bilayered graphene in "AA" stacking with the depicted area for holes and (b) such structure with created holes. The red arrows denote the atoms on a top layer that connect with the atoms on the bottom layer. In the lower figure the atomic connections are visible. R_h and D_h are the two geometrical parameters which define the structure, see the text for details. (c) Energy barrier calculated for the (3, 8) structure versus the distance between edges of two graphene layers. E_0 - denotes the energy of the initial structure. In the inset the 3D view of the (3, 8) BGS is presented. (e) Relative energy between initial (edges are not connected) and final (edges are

connected) states of BGS structures with various values of D_h.

properties of BGS are directly related to their atomic geometry or more specifically with the size of the holes and the distance between them as well as the flattening of the region between the holes. [25] With an increasing hole size the whole structure tends to the geometry of a carbon nanotube network, which can display semiconducting properties, [39,40] whereas with increasing of the distance between the holes the geometry of the structure tends to that of the semimetallic bilayered graphene. According to these facts we classified BGS structures using two independent parameters: size of the holes R_h (the length of one edge of the hexagonal hole in the units of graphene unit cell in zigzag direction) and distance between holes D_h (in the units of graphene unit cell in armchair direction) (*Figure 1* b).

Figure 1 c shows the "relative energy" (energy difference between the transition and initial structures) as a function of the distance between the atoms on the adjacent edges in the two layers for a particular parameter pair (R_h = 3, D_h = 8). By the decreasing of the distance between the atoms on the adjacent edges of the holes the relative energy decreases and tends to the minimum value (~-0.16 eV/atom). The minimum of the relative energy corresponds to a structure with bond length between the carbon atoms from neighboring layers equal to 1.415 Å. Such value of the bond length matches well with the equilibrium bond length between sp^2 carbon atoms. Further decreasing of the distance leads to a sharp increase of the energy. This fact allows us to conclude that in the absence of impurities on the edges of the holes the connected layers (BGS) form a stable configuration.

It should be noted that the spontaneous formation occurs not only for the "AA" stacked bigraphene (which is less favorable in energy) but also for the more favorable Bernal stacked BGS. Bernal stacked bilayered graphene with periodically arranged holes without the connections between the layers means that the holes were made in "AA" stacked graphene and then the layers were shifted. Only in a case when the distance between the holes was larger than the size of the holes the connections between the layers took place after the stacking transformation from "AB" to "AA" by means of the shifting of the layers

relative to each other with further formation of the bonds between the layers.

With the increasing of R_h the regions between the holes tend to become narrow zigzag graphene nanoribbons with edges of high chemical activity. This leads to the bending of the ribbon [38] with further decreasing of the distance between the layers and further formation of the chemical bonds between them. In both stacking at a fixed D_h, due to the increasing of R_h (size of the holes), the relative energy is negative in all the range of R_h which proves that the structures with connected layers (BGS) are the energetically preferable configurations.

Figure 1 e shows the relative energy as a function of the second parameter D_h (distance between the holes). With an increasing distance between the holes the relative energy increases and becomes positive. In that case the nanoribbons between the holes become wider and can't minimize their energy due to a bending, hence they remain flat. During the geometry optimization structure remains bilayered graphene without transformations from "AB" to "AA" stacking.

The pronounced dependence of the shape of the BGS upon the R_h and D_h parameters allows us to suppose a drastically different behavior of the electronic properties for the different structures. Indeed, we found that the variation of the parameters will allow to tune the conductivity from semiconducting to metallic. In order to explore this variation, we considered the electronic properties for a wide range of the structural parameters with the total number of atoms in unit cell from 150 to 1500.

In **Figure 2** a and **Figure 2** b the dependence of the band gap on the D_h parameter for structures with fixed R_h values of 2 and 3, respectively, are presented. We obtained that in both cases the band gap decreases with the increase of the distance between the holes (D_h), according to a quantum confinement law $E_{gap} \sim a_0 \dfrac{1}{(D_h)^n}$ (where a_0 and n are fitting coefficients). At the infinite limit of D_h the electronic structure tends to the bilayered graphene with zero band gap. At the presented values of R_h the fitting coefficients were obtained as a_0 = 0.43, n = 1.41 (**Figure 2** a) and a_0 = 0.11, n = 1.81 (**Figure 2** b), respectively.

In the case of the variation of R_h (size of the holes) at fixed D_h (**Figure 2** c) the behavior of the band gap

displays a more complex character, it also shows a decrease of the band gap by quantum confinement law $E_{gap} \sim a_1 \dfrac{1}{(R_h)^n}$ (where a_1 and n are the fitting coefficients). The slight oscillations can be attributed to the complex geometry of the structure (presence of nanotube Y-junctions which contain topological defects represented by 8-membered carbon rings) which strongly affects the electron distribution and the electronic properties of BGS. Obtained values of the fitting coefficients are $a_1 = 0.67$, $n = 0.76$.
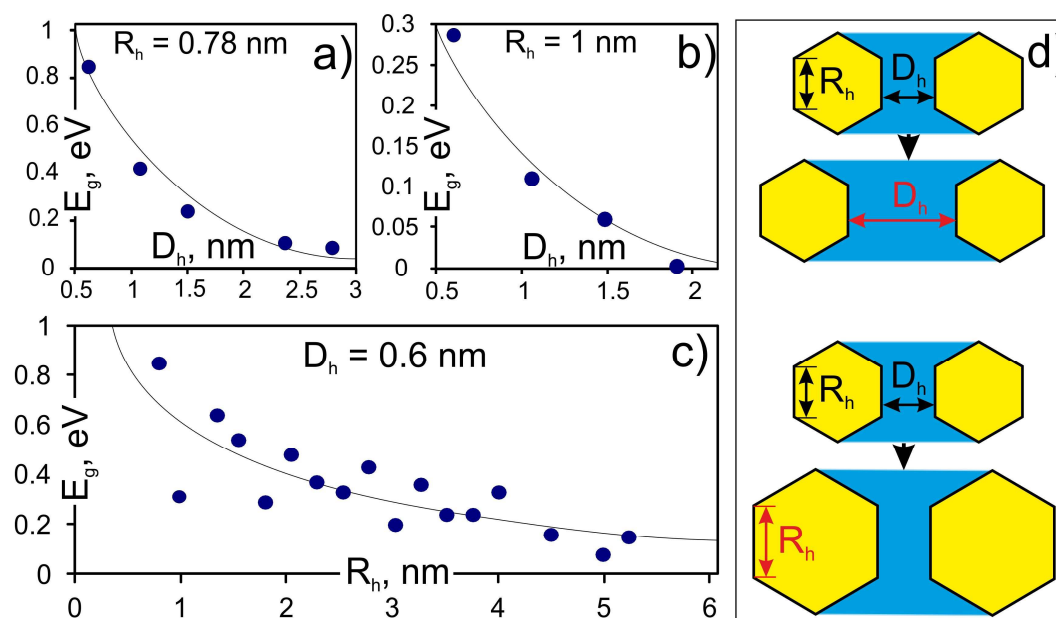

Figure 2 The dependence of the band gap on the two main parameters: (a-b) D_h, the distance between the holes and (c) R_h, the hole size. (d) The changing of the main parameters for (a, b) and (c).

It is important to notice that **Figure 2** shows the asymptotic limits of the two main parameters. In both cases the band gap tends to zero, because asymptotic limits of D_h and R_h correspond to geometries of metallic bilayered graphene and metallic armchair carbon nanotube (CNT), respectively. Note that in the earlier reports [41,42] bilayered graphene superlattices with rectangular unit cell were studied. All considered structures display semimetal properties besides noncovalent bonded bilayered nanomesh. [42]

It should be noted, however, that not only the structures with high values of R_h can have low values of the band gap. Decreasing of the size of the holes until point defects (vacancies) leads to an appearance of metallic properties without any dependence on the distance between the vacancies. This peculiar behavior of the band gap does not follow the dependence presented on the **Figure 2** c because point defects are not included in our classification. In the presented classification a BGS is described by means of the length of the edge of hexagonal holes in the zigzag direction, but the point defects cannot be described as hexagonal holes., This particular case, the unit cell of the bilayered graphene with point defects is presented in **Figure 3** a. **Figure 3** b shows the metallic band structure and the corresponding partial electron density of states (colored lines), as well as the total DOS (black line). Appearance of metallicity is originated from the intermediate hybridization state of the carbon atoms: the high curvature of the carbon lattice leads to a transition of the electronic states of the atoms marked by purple from sp^2 to sp^3 state, but the absence of the fourth neighbor for them creates a dangling bond with unsaturated conduction electron.
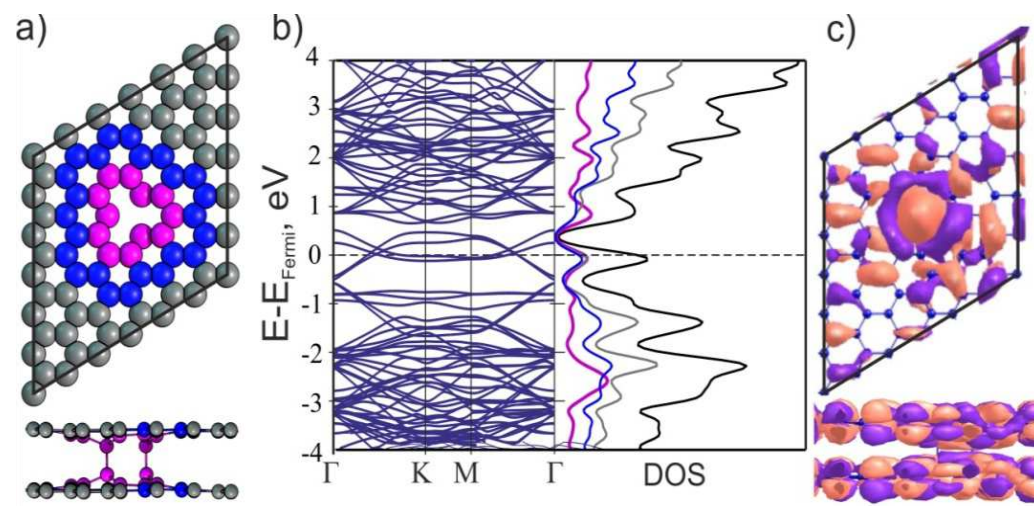
Figure 3 The BGS with point defect. a) Atomic structure of the unit cell of BGS with point defects (top and side view); b) band structure and density of states. Different colors show partial densities of states at the different atoms; c) the wave function distribution at the Fermi level with isovalue 0.03 electrons per cubic angstrom (top and side view, the two colors denote the positive and negative signs of the wave function).

From the **Figure 3** a and 3 b we can observe that the metallic behavior mainly originates from the atoms marked by purple (first neighbor atoms).

In order to investigate not only the electronic, but also the transport properties of the modeled BGS, we performed wave-packet dynamical (WPD) calculations. Two specific BGS with semiconductor and metallic properties were selected. **Figure 4** shows the model geometry, together with three snapshots from the time evolution of the probability density $\rho(\vec{r}, t)$, for the case of the semiconducting BGS. These 2D (XY) images illustrate the charge spreading on the top layer of the BGS. In the first frame at t = 0.2 fs the WP coming from the y direction (denoted by red arrows in **Figure 4** a) is still in the jellium electrode. At t = 3 fs a part of the WP has already penetrated about 2 nm into the BGS, while a part of it reflects back to the jellium electrode. By t = 12 fs the electrode has become empty and the WP spreads the whole BGS surface. Due to the finite energy spread of the initial WP, different energies are mixed in the snapshots of the time evolution (**Figure 4**).
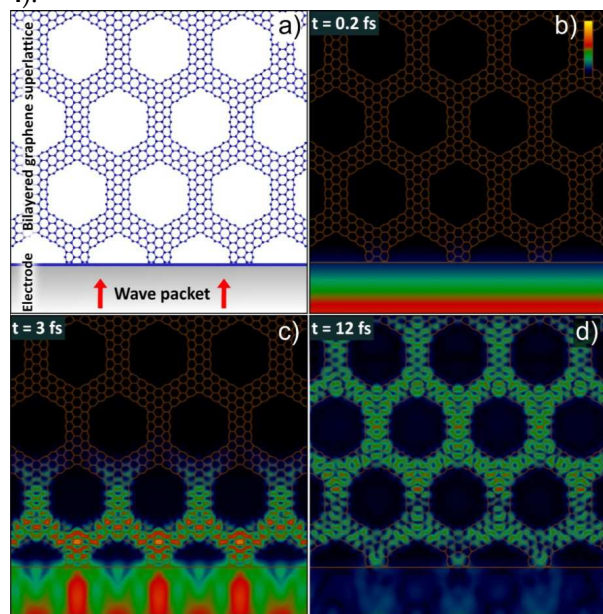

Figure 4 (a) Top view of the model geometry of the metallic electrode and the semi-infinite semiconducting BGS. (b-d) Selected snapshots from the time evolution of the probability density of the wave packet shown as color-coded 2D (top view XY) sections. Black corresponds to zero, yellow to the maximum density ($9.78 \cdot 10^{-5}$) [see the scalebar in (b)]. The size of the presentation window is 7.68 nm.

In order to study the dynamics at well defined energy values, we performed a time-energy (t → E) Fourier transform, thus we calculated $\psi(\vec{r}, E)$ from $\psi(\vec{r}, t)$. The probability current $j(\vec{r}, E)$ and the transmission function $T(E)$ is calculated from $\psi(\vec{r}, E)$. [34] **Figure 5** shows the probability density distributions and the corresponding transmission functions at the Fermi energy for the semiconductor and metallic BGS. In the semiconductor case the probability density shows a decay in the BGS (**Figure 5** a), and no further spreading occurs at the Fermi energy, opening a 0.6 eV transport gap. In contrast, the WP spreads along the whole metallic BGS with a high transmission probability.

The effect of the (CNT) Y-junctions on the electronic transport can be also seen in **Figure 5** b. Atomic structure of such kind of CNT Y-junctions were considered in Ref. [43] and called as "planar jungle gyms". The slightly decreased probability density at the junctions corresponds to the reduced DOS at the Fermi energy calculated by DFT.
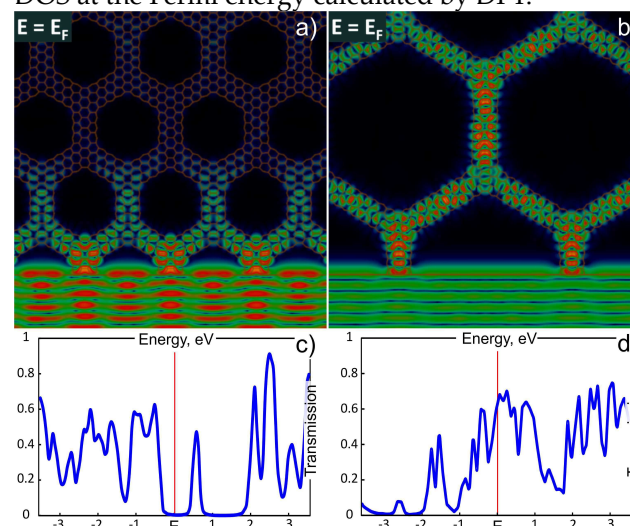

Figure 5 (a-b) Probability density on the semiconductor and metallic BGS at the Fermi energy shown by color-coded 2D (top view XY) sections. The images are renormalized individually to their maximum density. The maximum density values are $5.23 \cdot 10^{-5}$ and $1.31 \cdot 10^{-4}$ for the (a) and (b), respectively; (c-d) Transmission functions of the two BGS.

CONCLUSIONS. In this work we have studied in detail the novel hexagonal nanomeshes based on bilayered graphene. The atomic structure and the formation process were investigated using the density functional theory. It was found that after making holes in the bilayered graphene lattice, the two layers tend to connect with each other along

the edges of the holes without any activation barrier (in the case of absence of impurity atoms in the edges). Using the DFTB approximation the electronic properties of the BGS and the dependences of the band gap on two main parameters characterizing the geometry were studied in detail. In the asymptotic case, for both parameters the band gap tends to zero. Also a special case of the metallic BGS with point defects was considered. Electron transport through different BGS was calculated by the wave packet dynamical method. The results confirm the semiconductor and metallic properties. The presented results can serve as a basis for the further investigation and fabrication of jointless (absence of stacking faults) hollow semiconducting materials with tunable electronic properties, with potential applications in mobility nanoelectronic devices.

Acknowledgements

References

[1] Novoselov, K. S.; Geim, A. K.; Morozov, S. V.; Jiang D; Zhang Y; Dubonos, S. V.; Grigorieva, I. V.; Firsov, A. A. Electric Field Effect in Atomically Thin Carbon Films. *Science* **2004,** *306,* 666-669.

[2] Novoselov, K. S.; Jiang, D.; Schedin, F.; Booth, T. J.; Khotkevich, V. V.; Morozov, S. V.; Geim, A. K. Two-dimensional Atomic Crystals. *Proc. Nat. Acad. Sci.* **2005,** *102,* 10451-10453.

[3] McCann, E.; Koshino, M. The Electronic Properties of Bilayer Graphene. *Rep. Prog. Phys.* **2013,** *76,* 056503(28).

[4] McCann, E.; Fal'ko, V. I. Landau-level Degeneracy and Quantum Hall Effect in a Graphite Bilayer. *Phys Rev Lett* **2006,** *96,* 086805-086808.

[5] Chernozatonskii, L. A.; Sorokin, P. B.; Brüning, J. W. Two-dimensional Semiconducting Nanostructures Based on Single Graphene Sheets with Lines of Adsorbed Hydrogen Atoms. *Appl. Phys. Lett.* **2007,** *91,* 183103-183105.

[6] Chernozatonskii, L. A.; Sorokin, P. B.; Belova, E. É.; Brüning, J.; Fedorov, A. S. Superlattices Consisting of "lines" of Adsorbed Hydrogen Atom Pairs on Graphene. *JETP Lett.* **2007,** *85,* 77-81.

[7] Chernozatonskii, L. A.; Sorokin, P. B. Nanoengineering Structures on Graphene with Adsorbed Hydrogen "lines". *J. Phys. Chem. C* **2010,** *114,* 3225-3229.

[8] Castro, E. V.; Novoselov, K. S.; Morozov, S. V.; Peres, N. M. R.; Santos, J. M. B. L. D.; Nilsson, J.; Guinea, F.; Geim, A. K.; Neto, A. H. C. Biased Bilayer Graphene: Semiconductor with a Gap Tunable by the Electric Field Effect. *Phys. Rev. Lett.* **2007,** *99,* 4.

[9] Liu, X.; Zhang, Z.; Guo, W. Universal Rule on Chirality-dependent Bandgaps in Graphene Antidot Lattices. *Small* **2013,** *9,* 1405-1410.

[10] Pedersen, T. G; Flindt, C.; Pedersen, J.; Jauho, A. P.; Mortensen, N. A.; Pedersen, K. Optical Properties of Graphene Antidot Lattices. *Phys. Rev. B* **2008,** *77,* 6.

[11] McCann, E. Asymmetry Gap in the Electronic Band Structure of Bilayer Graphene. *Physical Review B* **2006,** *74,* 161403(R)-161406(R).

[12] Nemes-Incze, P.; Magda, G.; Kamarás, K.; Biró, L. P. Crystallographically Selective Nanopatterning of Graphene on SiO$_2$. *Nano Research* **2010,** *3,* 110-116.

[13] Dobrik, G; Nemes-Incze, P.; Tapasztó, L.; Lambin, P.; Biró, L. P. Nanoscale Lithography of Graphene with Crystallographic Orientation Control. *Physica E: Low-dimensional Systems and Nanostructures* **2012,** *44,* 971-975.

[14] Lee, J. H.; Jang, Y.; Heo, K.; Lee, J. M.; Choi, S. H.; Joo, W. J.; Hwang, S. W.; Whang, D. Large-scale Fabrication of 2-D Nanoporous Graphene Using a Thin

Anodic Aluminum Oxide Etching Mask. *J Nanosci Nanotechnol* **2013,** *13*, 7401-7405.

[15] Zubeltzu, J.; Chuvilin, A.; Corsetti, F.; Zurutuza, A.; Artacho, E. Knock-on Damage in Bilayer Graphene: Indications for a Catalytic Pathway. *Physical Review B* **2013,** *88*, 245407-245417.

[16] Bai, J.; Zhong, X.; Jiang, S.; Huang, Y.; Duan, X. Graphene Nanomesh. *Nature Nanotech.* **2010,** *5*, 190-194.

[17] Dvorak, M.; Oswald, W.; Wu, Z. Bandgap Opening by Patterning Graphene. *Scientific Reports* **2013,** *3*, 2289-2295.

[18] Pedersen, T. G.; Flindt, C.; Pedersen, J.; Mortensen, N. A.; Jauho, A. P.; Pedersen, K. Graphene Antidot Lattices: Designed Defects and Spin Qubits. *Phys. Rev. Lett.* **2008,** *100*, 4.

[19] Ouyang, F.; Peng, S.; Liu, Z.; Liu, Z. Bandgap Opening in Graphene Antidot Lattices: the Missing Half. *ACS Nano* **2011,** *5*, 4023-4030.

[20] Fürst, J. A.; Pedersen, J. G.; Flindt, C.; Mortensen, N. A.; Brandbyge, M.; Pedersen, T. G.; Jauho, A. P. Electronic Properties of Graphene Antidot Lattices. *New Journal of Physics* **2009,** *11*, 095020-095036.

[21] Sinitskii, A.; Tour, J. M. Patterning Graphene Through the Self-assembled Templates: Toward Periodic Two-dimensional Graphene Nanostructures with Semiconductor Properties. *J. Am. Chem. Soc.* **2010,** *132*, 14730-14732.

[22] Kim, M.; Safron, N. S.; Han, E.; Arnold, M. S.; Gopalan, P. Fabrication and Characterization of Large-area, Semiconducting Nanoperforated Graphene Materials. *Nano Lett.* **2010,** *10*, 1125-1131.

[23] Liu, Z.; Suenaga, K.; Harris, P. J. F.; Iijima, S. Open and Closed Edges of Graphene Layers. *Phys. Rev. Lett.* **2009,** *102*, 015501-015504.

[24] Campos-Delgado, J.; Kim, Y. A.; Hayashi, T.; Morelos-Gómez, A.; Hofmann, M.; Muramatsu, H.; Endo, M.; Terrones, H.; Shull, R. D.; Dresselhaus, M. S. *et al.* Thermal Stability Studies of Cvd-grown Graphene Nanoribbons: Defect Annealing and Loop Formation. *Chemical Physics Letters* **2009,** *469*, 177-182.

[25] Algara-Siller, G.; Santana, A.; Onions, R.; Suyetin, M.;

Biskupek, J.; Bichoutskaia, E.; Kaiser, U. Electron-beam Engineering of Single-walled Carbon Nanotubes from Bilayer Graphene. *Carbon* **2013,** *65*, 80-86.

[26] Zhan, D.; Liu, L.; Xu, Y. N.; Ni, Z. H.; Yan, J. X.; Zhao, C.; Shen, Z. X. Low Temperature Edge Dynamics of Ab-stacked Bilayer Graphene: Naturally Favored Closed Zigzag Edges. *Scientific Reports* **2011,** *1*, 12-16.

[27] Soler, J. M.; Artacho, E.; Gale, J. D.; García, A.; Junquera, J.; Ordejón, P.; Sánchez-Portal, D. The Siesta Method for *Ab Initio* Order-N Materials Simulation. *Journal of Physics: Condensed Matter* **2002,** *14*, 2745-2779.

[28] Monkhorst, H. J.; Pack, J. D. Special Points for Brillouin-zone Integrations. *Phys. Rev. B* **1976,** *13*, 5188-5192.

[29] Elstner, M.; Porezag, D.; Jungnickel, G.; Elsner, J.; Haugk, M.; Frauenheim, T.; Suhai, S.; Seifert, G. Self-consistent-charge Density-functional Tight-binding Method for Simulations of Complex Materials Properties. *Physical Review B* **1998,** *58*, 7260-7268.

[30] Garraway, B. M.; Suominen, K. A. Wave-packet Dynamics: New Physics and Chemistry in Femto-time. *Reports on Progress in Physics* **1995,** *58*, 365-419.

[31] Vancsó, P.; Márk, G. I.; Lambin, P.; Mayer, A.; Hwang, C.; Biró, L. P. Effect of the Disorder in Graphene Grain Boundaries: a Wave Packet Dynamics Study. *Applied Surface Science* **2014,** *291*, 58-63.

[32] Mayer, A. Band Structure and Transport Properties of Carbon Nanotubes Using a Local Pseudopotential and a Transfer-matrix Technique. *Carbon* **2004,** *42*, 2057-2066.

[33] Mayer, A. Transfer-matrix Simulations of Electronic Transport in Single-wall and Multi-wall Carbon Nanotubes. *Carbon* **2005,** *43*, 717-726.

[34] Vancsó, P.; Márk, G. I.; Lambin, P.; Mayer, A.; Kim, Y. S.; Hwang, C.; Biró, L. P. Electronic Transport Through Ordered and Disordered Graphene Grain Boundaries. *Carbon* **2013,** *64*, 101-110.

[35] Márk, G. I.; Biró, L. P.; Gyulai, J. Simulation of Stm Images of Three-dimensional Surfaces and Comparison with Experimental Data: Carbon Nanotubes. *Physical Review B* **1998,** *58*, 12645-12648.

[36] Márk, G. I.; Vancsó, P.; Hwang, C.; Lambin, P.; Biró, L. P. Anisotropic Dynamics of Charge Carriers in Graphene. *Physical Review B* **2012,** *85*, 125443-125451.

[37] Scuracchio, P.; Dobry, A. Bending Mode Fluctuations and Structural Stability of Graphene Nanoribbons. *Physical Review B* **2013,** *87*, 165411-165417.

[38] Kit, O. O.; Tallinen, T.; Mahadevan, L.; Timonen, J.; Koskinen, P. Twisting Graphene Nanoribbons into Carbon Nanotubes. *Physical Review B* **2012,** *85*, 085428-085434.

[39] Bekyarova, E.; Itkis, M. E.; Cabrera, N.; Zhao, B.; Yu, A.; Gao, J.; Haddon, R. C. Electronic Properties of Single-walled Carbon Nanotube Networks. *J. Am. Chem. Soc.* **2005,** *127*, 5990-5995.

[40] Timmermans, M. Y.; Estrada, D.; Nasibulin, A. G.; Wood, J. D.; Behnam, A.; Sun, D. M.; Ohno, Y.; Lyding, J. W.; Hassanien, A.; Pop, E. *et al.* Effect of Carbon Nanotube Network Morphology on Thin Film Transistor Performance. *Nano Research* **2012,** *5*, 307-319.

(41) Demin V A ; Chernozatonskii L A Nanotube Connections in Bilayer Graphene with Elongated Holes. *Nanomaterials: Application & Properties* 03NCNN32-03NCNN34 , Alushta, the Crimea, Ukraine, 2013).

[42] Chernozatonskii, L. A.; Demin, V. A.; Artyukh, A. A. Bigraphene Nanomeshes: Structure, Properties, and Formation. *JETP Letters* **2014,** *99*, 309-314.

[43] Chernozatonskii, L. A. Carbon Nanotube Connectors and Planar Jungle Gyms. *Physics Letters A* **1992,** *172*, 173-176.